A SEVENTY NINE DAY'S TIME-SERIES OF BLACK SEA COASTAL OZONE, AEROSOL, AND METEOROLOGICAL PARAMETERS: STATISTICAL INTER-RELATIONSHIPS, AND IMPLICATIONS

D. M. Ivanov[1], D. G. Lazarov[1], A. P. Blagoev[1], V. C. Danchovski[1], E. H. Donev[1] and Bo L.B. Wiman[2]

[1] Department of Meteorology and Geophysics, Faculty of Physics, Sofia University, Bul. James Bourcher No 5, Sofia1164, Bulgaria
[2]Environmental Science and Technology Section, School of Natural Sciences, Linnaeus University, Sweden

Abstract. This paper applies a variety of statistical methods for exploring relationships between time series of ground-level ozone concentrations, aerosols (in terms of number-concentrations of particles larger than 0.5 μm) and meteorological parameters. The time sequences were obtained automatically and simultaneously (records of the every hour averages) at a coastal station near Ahtopol in Bulgaria for the period May 10 - July 27, 2002. Introductory statistical analyses suggested a number of potential interrelationships between ozone concentration variations and some meteorological parameters. There were also indications of aerosol-particle concentrations showing some connections with wind speed and wind direction, and also with solar radiation; the latter relationship however likely to be a result of the partly radiation-driven pattern for wind speed and direction. These introductory findings warranted the use also of Mathematical Spectral Analysis (MSA) in analysing the time series, so as to show the usefulness of MSA for meteorological applications. The conclusions based on the power spectra, the cross-amplitude spectrum, the absolute coherency spectrum and the phase spectrum are confirmed by the diurnal cycles. The power spectrum of the observed data as well as the cross-amplitude, absolute coherency and phase spectra were calculated for hourly meteorological parameters, aerosols and ozone data. The present article contains the calculations of the spectra and their interpretation. Among conclusions is that diurnal variations of meteorological parameters well explain diurnal variation of ozone concentrations, but that the daily aerosol concentrations variations are less affected by diurnal variability of meteorological parameters except solar radiation.

Keywords: coastal-zone meteorology, ground-level ozone, particle-number concentrations, mathematical cross-spectrum analysis

Introduction

Relationships between ground-near ozone and aerosols (suspensions of liquid or solid particles in the atmosphere with particle sizes ranging from about 0.01 μm to several tens of μm) are being subject to increasing scientific interest for several reasons (e.g, Bonasoni et al,. 2004). Both components exert effects on human health and on the vitality of forests and agricultural crops (e.g., Houthuijs et al., 2001; Karnosky et al., 2003; Fowler et al., 2009). In addition, ozone and aerosols both affect climate (IPCC, 2007) although in most respects with opposite influences on radiative forcing (see Table 1 for a list of abbreviations). Because of the continuous production of ozone precursors, in particular in urban regions, the current global contribution of tropospheric ozone to the anthropogenic part of the greenhouse effect is substantial (ca 10%). Aerosols, however – emanating from a multitude of natural as well as anthropogenic sources, such as wind-erosion of soils, bubble-bursting at the sea/air interface, and conversion of trace gases into particles (e.g., Wiman et al., 1990; Andreae and Crutzen, 1997; Seinfeld and Pandis, 1998) – affect climate in more complex ways. The mechanisms include direct and indirect forcing (e.g., IPCC 2007). Most types of aerosols scatter sunlight back into space – they have a direct cooling effect by reducing the amount of solar radiation that reaches the Earth's surface. Some aerosol types, however, have a substantial imaginary part in their refractive index, and can therefore absorb sunlight and generate warming. The indirect effect involves aerosol particles acting as (additional) cloud condensation nuclei. Clouds thus created will in most cases cool the Earth's surface. The effect of aerosols, therefore, is in general opposite to the effect of tropospheric ozone and the several other greenhouse gases (IPCC, 2007). However, because of their low residence times, tropospheric ozone and aerosols have important, but complex, spatial climate-change effects, influencing local and regional climates. This is in contrast to other radiatively active substances which mix vertically and laterally in the global atmosphere.

Hence, the interactions between tropospheric ozone and aerosols are of particular interest from aspects of health, ecosystem biogeochemistry, and climate change. The interactions, however, need much further research. Among important examples are gas-to-particle conversion processes such as the catalytic and photochemical transformation of sulphur oxides (such as emitted by volcanoes and human burning of fossil fuels) into sulphate particles. Sulphate aerosols may significantly influence ozone loss via chemical processes as well as physically such as through affecting the illumination time of solar radiation driving ozone generation and decay mechanisms. In addition, certain types of non-methane hydrocarbons (terpenoids, isoprenes, and others) are emitted by forests and then transform into aerosol particles through photochemically driven processes (e.g., Seinfeld and Pandis, 1998; Paulot et al., 2009). Some of these processes involve tropospheric ozone as well as anthropogenic trace gases (such as nitrogen oxides emitted by traffic systems). Also, a number of reactions between sea-salt aerosols and the formation of ground-near ozone are of importance. For instance, Knipping and Dabdub (2003) suggest that the inclusion of sea-salt-derived chlorine chemistry is of high interest to advancing the understanding of coastal ozone formation and decay. This is because chlorine might increase predicted morning ozone concentrations by as much as 12 ppb in coastal regions and by 4 ppb in the peak domain ozone in the afternoon.

These and many other factors influence ozone and aerosol concentrations. Among important meteorological parameters in that context are solar radiation, temperature and relative humidity.

In the current contribution, we investigate time series of 79 days of ozone, aerosols, solar radiation, temperature, relative humidity (RH), and wind speed and direction, at a Bulgarian costal site, Ahtopol (Lat 42°00' N, Long 28°01' E). We study the pattern of variation of, and between, these parameters with several statistical tools, including Spectral Analysis, MSA. Hence, power spectra, coherency spectra, phase spectra and for various pairs of parameters are included in the analysis. Our objectives are to help advance the understanding of relationships between aerosols, ozone and meteorology; these are key factors in choosing the right variables for ozone-predicting models (Alexandrov et al., 2005). In addition, our aim is to show how some common statistical tools can be efficiently complemented by MSA.

Table 1. List of abbreviations.

IPCC	Intergovernmental Panel on Climate Change
LPC	Laser Particle Counter
MRI	Meteorology Research Incorporation
ppb	part per billion
ppb(v)	part per billion by volume
RH	Relative Humidity

Site, equipment, data acquisition and statistical procedures

The monitoring site is about 200 meters from the shore, about 2 km south of the town of Ahtopol, on the Black Sea coast NE of the Strandzha low-elevation mountain region. The climate in the Ahtopol region is slightly different from the rest of the Bulgarian sea coast and is mild and strongly influenced by the Mediterranean. The research station is located in a low-pollution region and should serve fairly well as a rural-type background site (cf. Wiman et al., 2007). Diurnal cycles of aerosol and ozone concentrations in the region are influenced by the local sea/land breeze circulation which, however, is modified by the circulation in the nearby low-elevation Strandzha mountain region (Skakalova et al., 2003). This region is characterised by vast expanses of oak forests (for details, see Wiman and Gaydarova,2008) which can function as sources of several organic compounds involved in the formation of ozone.

The time-series data were collected in 2002 from May 10, 5 p.m. (Local Standard Time) to July 28, 1 p.m. Ozone and aerosol concentrations were measured together with wind speed and direction, temperature and RH, and total solar radiation as detailed in Table 2. For the scope of the present study we explore ozone and aerosol concentrations at 1 m height and solar radiation, temperature, RH, wind speed and direction at 5 m. Data were logged by a Campbell Scientific 21x unit, and then processed into hourly averages. Aerosol-particle number concentrations were measured with a Laser-based Particle Counter (LPC; Climet 4010) re-designed to provide a continuous analogue output signal proportional to the sum of concentrations in the two channels instead; thus providing the

concentration of particles with diameter > 0.5 µm. Very many measurements have been performed with LPC devices in the region (see Wiman et al., 1999a; 1999b) and show that the sub-interval > 5 µm contains only a small fraction (less than 5%) of the concentration of particles > 0.5 µm; hence, our LPC data here essentially refer to the 0.5 to 5 µm particle size class. Although that class provides only limited information on sub-µm particles (which are of importance to ozone-aerosol interactions) it tracks the general features of variations in the accumulation aerosol mode fairly well (cf., Whitby, 1978). Also, and by definition, the LPC does not give information on aerosol chemistry. However, such data from the region are available from a month-by-month sampling programme over the period summer 1998 to summer 2000 (Wiman et al., 2007) and from some campaigns (Wiman et al., 2002), and offer some comparative information. Inter alia, concentrations levels of S, Cl, V, Zn and Se were found to be substantially higher in the Ahtopol region than in high-elevation mountain areas in Bulgaria.

Table 2. Information on the equipment used and the parameters measured at the Ahtopol station. Data were recorded on time scales of the order of minutes; for this contribution they were processed into hourly averages.

sensor	Parameter	height	units
LPC Climet 4010	Concentrations of particles larger than 0.5 µm in diameter*	1 m	particles cm^{-3}
Teco 49	O_3 concentrations	1 m	ppb
VAISALA WAA12	Wind Speed	5 m	$m\ s^{-1}$
VAISALA WAV12	Wind Direction	5 m	degrees
Eppley	Total Solar Radiation**	5 m	$W\ m^{-2}$
MRI	Precipitation	1 m	mm
Vaisala HMP35C	Temperature	5 m	^{o}C
Vaisala HMP35C	Relative Humidity	5 m	%

*in this study calculated from readings in mV.

** this instrument measures over the 285 to 2800 nm optical spectral range.

The data set was first explored with various common statistical techniques so as to help provide a first-level insight into the interrelationships. Since these introductory analyses turned out to warrant in-depth study of potential cycles we also explored the data set with spectral methods (in this case using all 1893 hours of measurements). For the objectives of this work, we applied spectral analysis based on Parseval's relation (Priestley, 1981; Brockwell and Davis, 1991). It presents the power spectrum as the decomposition of the total variance into frequency-dependent components. The cross-amplitude spectrum between two time series provides an assessment of the frequency range where the two time series exhibit best mutual fit. The absolute coherency spectrum can be used to measure the linear correlation between two time series for all frequencies. It is analogous to the correlation coefficient, and signifies whether some periodic pattern occurs in both time series. However, the absolute coherency spectrum does not specify whether they are

synchronized in time. This information is instead available from the phase spectrum. After calculating the spectra of time series, a common result is that most of the power is concentrated in one or a few narrow bands, thus masking the spectral estimates in the bands where the power is small. Therefore, in order to improve those spectral estimates, digital filtering of the data is needed. In this work a cosine filter is used with half-of-lag period sized 15 hours and with the correlation window width 30 hours. The time step for the calculations is 1 hour. The width chosen for the correlation window is due to the length of the time series, and is also considered appropriate because daily variations are the main target of the present study. Choosing a relevant width of the correlation window is of great importance because the values selected might affect the outcome.

Results and discussion

Introductory overview and relationships

We first present the data sequences in graphic form (Fig. 1) and explore some of their basic features. For our purposes here, the data sequence for each parameter was normalized to the maximum range (i.e., to the [max-min]-value in each respective parameter sequence) occurring over the 78 days of continuous measurements.

From Fig. 1 several basic patterns emerge. Among them are, as expected, the strong connections between solar radiation, temperature, and RH. The two latter parameters co-vary with no essential mutual phase shift, but are both somewhat time-shifted (lagging behind by about 1 hour) vis-à-vis solar radiation. Ozone concentrations also relate strongly to solar radiation, but with a phase-shift of around 2 hours' delay during the morning, and reaching their peaks about 4-5 hours later than does radiation. These connections are more clearly observable when the average 24-hours patterns are calculated for solar radiation, temperature, RH, and ozone concentrations and based on normalization of each parameter to its maximum range in the respective sequences of 24-hour means; cf. Fig. 2. Relationships between wind velocities and radiation, temperature, and RH seem to exist as well (see Fig. 2). However, the connections are weaker, as should be expected because of the influence of several other factors, including sub-periods of dominance of synoptic weather situations as well as the effects of landscape topography on the sea/land circulation. As also shown in Fig. 2, aerosol particle concentrations have an average tendency to increase in daytime although the variability (such as in terms of standard deviations of the respective hourly means) is high, making connections with other parameters more difficult to assess. It needs to be observed that the respective hourly means are associated with large variation (provided in terms of standard deviations in the Fig. 2 caption). Inevitably, a substantial fraction of this variation, in particular for radiation and radiation-driven parameters, derives from the change in day-length over the May 10 to July 27 period. This variation necessitates the use of various forms of mathematical spectral analysis, dealt with in next section.

Studying the effects of wind direction necessitates polar coordinates. Fig. 3a presents the distribution of wind directions, and Fig. 4 the variation of wind velocity with wind direction. Fig. 3a confirms that winds from the SW (land areas) and N to NNE (sea

areas) dominate, while Fig. 4 shows that wind speeds reach high values more often in the N-to-NE sector than in the S-to-W sector. Additional statistical analyses indicate that three basic categories of wind circulation occurred during the measurement period (May 10 to July 27). The categories share approximately similar fractions of the sequence. They contain (cf. Fig. 3b) fairly typical land/sea circulation patterns, a somewhat more complex pattern probably resulting from the influence of the nearby mountain-valley systems, and a highly shifting pattern likely to involve front passages and other synoptic features.

It is then of interest to explore how ozone and aerosol-particle concentrations vary with wind direction; see Fig. 5 and Fig. 6, respectively. Ozone concentration variations show weak, if any, connections with wind directions, while there is a tendency for higher particle concentrations occurring more often in air masses emanating from the sea than in those coming from the land. Comparing Fig. 6 (particle-concentration distribution with wind direction) with Fig. 4 (wind-velocity distribution with wind direction) suggests some similarities. These are brought out by Fig. 7, wherein the distribution of particle flux (concentration times wind velocity) with wind direction is shown.

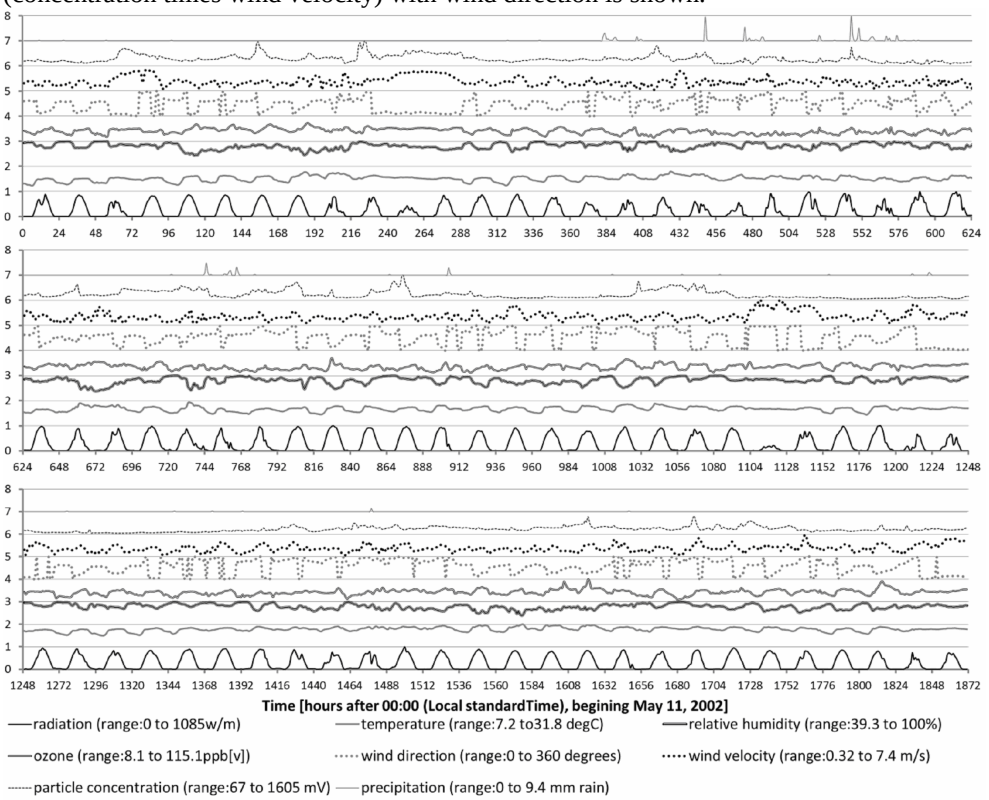

Fig. 1. Overview of the data series. The diagram is constructed such that each respective parameter is normalised to its maximum range over the measurement period (78 days). Each parameter is then plotted as a function of time in a diagram field spanning the vertical interval 0 to 1. The field denoted "0" shows solar radiation, field "1" shows temperature, field "2" relative humidity, field "3" ground-level ozone concentrations, field "4" wind direction, field "5 wind velocity, field "6" particle

concentrations, field "7" precipitation. Legends in the diagram provide information on the respective spans used in the normalisations. For particle-number concentrations, the mV range given corresponds to the range 0.6 . 103 to 14 . 103 particles per litre (particle sizes > 0.5 µm, with particles in the interval 0.5 to 5 µm strongly dominating).

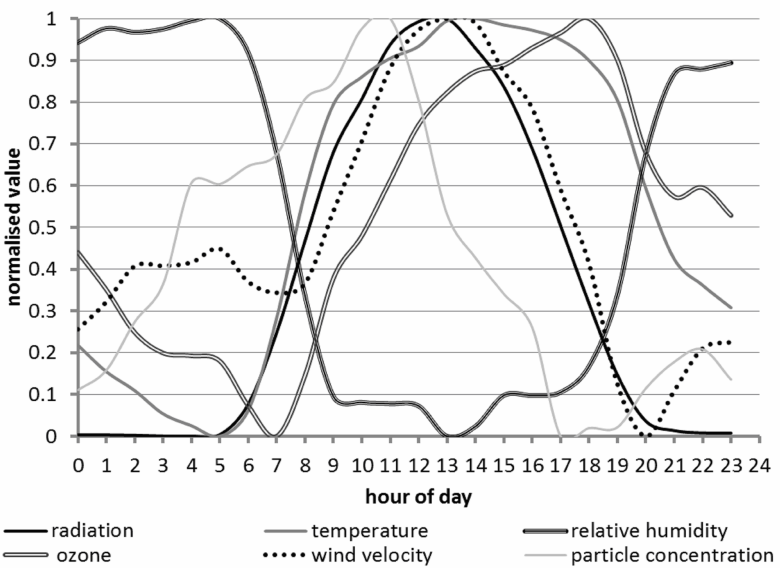

Fig. 2. Average 24-hours patterns for solar radiation, temperature, relative humidity (RH), ozone (O3) concentrations, wind velocity and concentrations of aerosol particles > 0.5 µm. In order to bring out the variations in one diagram, all parameters have be been normalized to their respective maximum ranges.

These introductory analyses of the data set suggest a number of connections, and time-lags, between the meteorological parameters as such (solar radiation, temperature, relative humidity, wind speed, and wind direction). They also suggest that interrelationships, and lead/lags, exist between ground-near ozone concentration variations and some meteorological parameters (solar radiation and temperature in particular). Relationships between ozone concentrations and wind direction seem weak, however. Aerosol-particle concentrations (and fluxes) show some connections with wind speed and wind direction, and also with solar radiation; the latter relationship however likely to be a result of the partly radiation-driven pattern for wind speed and direction. Relationships between ozone concentrations and particle concentrations may exist, but, if so, seem weak. Although, as discussed in the Introduction, interactions between ozone formation/decay and aerosols can be assumed to exist, our data suggest that such interactions mostly do not occur in particle-size ranges above 0.5 µm (i.e., in size ranges captured by the LPC deployed in this study).

Naturally, the indications of time lags between several parameters show that standard correlation procedures are not relevant in the further analysis. Instead, we now turn to spectral-analysis methods.

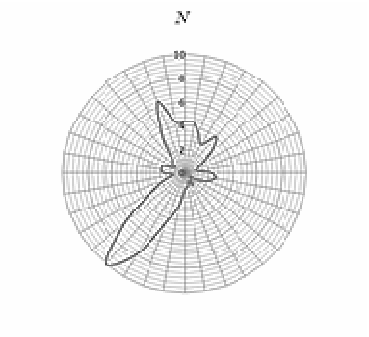

Fig. 3a. Wind-direction distribution (so called Wind Rose, percent per 10-degree bins of total counts).

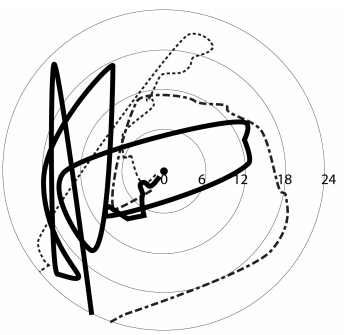

Fig. 3b. Illustration of three main types of wind circulation in the data sequence. Circles denote time of the day. Each line starts at midnight, and the evolution is then given on an hourly basis. Type 1 (long/short dashes): fairly typical land/sea circulation pattern, with the wind coming from the SW direction from about midnight, then in the morning (around 6 a.m.) shifting to a W to NSW to N wind (around noon), and then further on to a W wind (around 6 p.m.), reaching the SW direction again around midnight. Type 2 (short dashes): the circulation occurs mainly in the NE, NW, and SE quadrants. Type 3 (solid line): the evolution of a more complex circulation pattern.

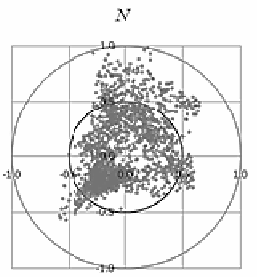

Fig. 4. Wind speeds (normalized to maximum over the period, 7.4 ms-1), distribution with wind direction. Circles give the normalized wind speeds; negative values are used for wind velocities pertaining to winds from the S to W quadrant, positive values for the N to E quadrant; positive (negative) and negative (positive) values pertain to winds from the E to S (W to N) quadrants.

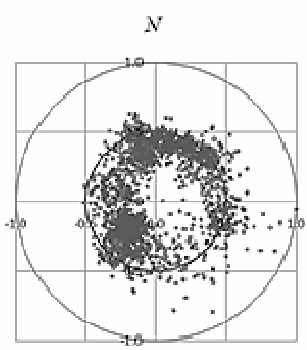

Fig. 5. Ozone concentrations (normalised to maximum over the period, 115 ppb(v), distribution with wind direction.

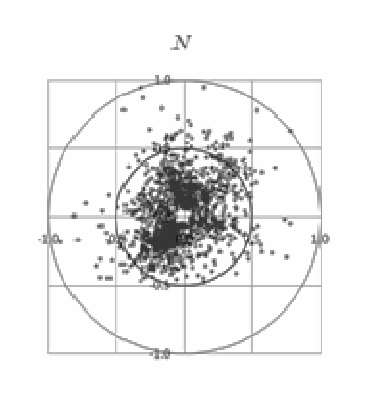

Fig. 6. Particle concentrations (normalised to maximum over the period, 14 ^{x} 10^{3} particles larger than 0.5 µm in size per litre), distribution with wind direction.

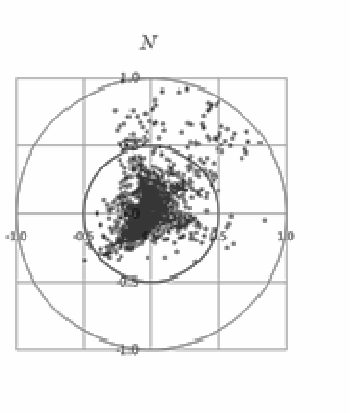

Fig. 7. Aerosol-particle fluxes (normalised to maximum over the period, 51 particles larger than 0.5 µm in size per m^2 and s), distribution with wind direction.

Spectral analyses

The programme used here (Donev et al., 1977, 1979, 1986; Zeller et al., 2001) works simultaneously on two time series of elements. In addition to providing autocorrelation and auto spectral analysis the programme runs a cross-spectral treatment of the data. The main objective of this part of the data analyses was to obtain spectra for periods between 24 and 2 hours.

Auto-spectra and cross-spectra were obtained according to Table 3.

Table 3. Pairs studied in the spectral analysis. Graphs pertaining to each pair are given by Figure numbers in the table.

	ozone concentration	particle concentration
radiation	Fig. 8a,b	
relative humidity	Fig. 9a,b	Fig. 10a,b
wind velocity		Fig. 11a,b
ozone concentrations		Fig. 12a,b

The Ozone-Radiation pair. The maximum power of the ozone is for the 24-hours period. The absolute coherency spectra (Fig. 8a) show a very good coherence for the 24-hours period whereas 8 and 6 hour periods show weaker coherence. The coherence for shorter periods is not statistically significant. The ozone's phase lag is 4 hours for the 24-hours period and almost 2 hours for the 8 and 6 hours periods (Fig.8b).

The Ozone – Relative Humidity pair. The absolute coherency spectra (Fig. 9a) show a very good coherence for the 24-hours period whereas 8, 4.8, 3.5, 2.7, and 2.18 hour periods show weaker coherence. The phase-lag for RH (cf. Fig. 9b) is about 2 hours for the

periods of 3.5 and 4.8 hours, about 3.6 hours for 8-hours period and for a 24-hours period almost 10 hours. However, the dependency is not linear. This analysis is confirmed by the daily trends (Fig. 2) where the coherence clearly emerges.

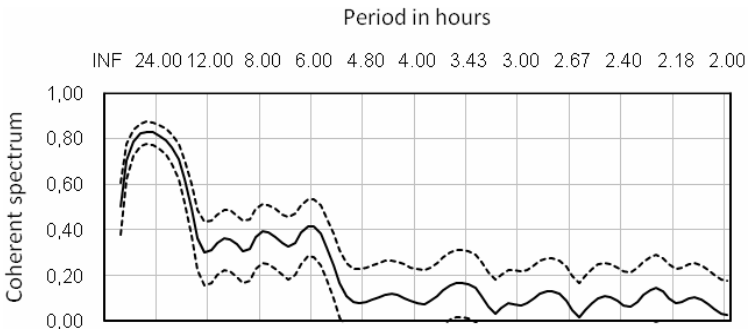

Fig. 8a. Absolute coherency spectrum for the ozone (ppb) and solar-radiation (W m^{-2}) time series.

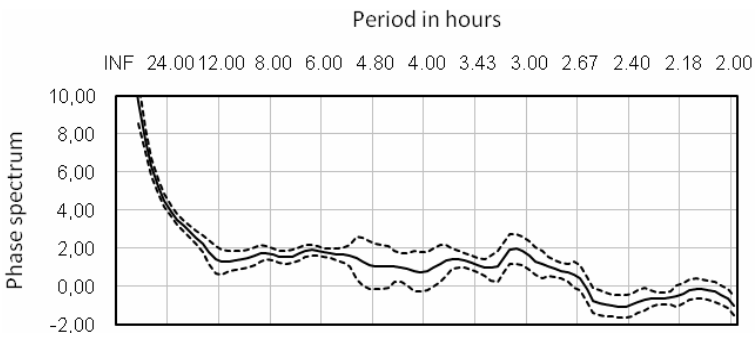

Fig. 8b. Phase spectrum for the ozone (ppb) and solar-radiation (W m^{-2}) time series.

The particle-concentration – Relative Humidity pair. The largest significant coherence (Fig. 10a) is for the 4 hour period. There are smaller ones as well for the 16, 8, 3.25, 2.8 and 2.5 hour periods. There is not a strong dependency for the 24-hour period. We suggest that the 8-hour period can be linked to inflows of moist air from the sea or a dry air from the mainland, not in the least because of the RH effects on growth and decline of maritime aerosols (e.g., Wiman, 2000; Foltescu et al., 2005). The phase spectrum (Fig. 10b) shows that the two parameters are almost synchronous for periods smaller than 12 hours. For longer periods the confidence interval (dotted lines) becomes wider, thwarting reliable conclusions. The daily trend graphics (cf. Fig. 2) shows the concurrence of the aerosol concentration maximum with the minimum value of RH, and the concurrence of lower aerosol concentration and higher RH values.

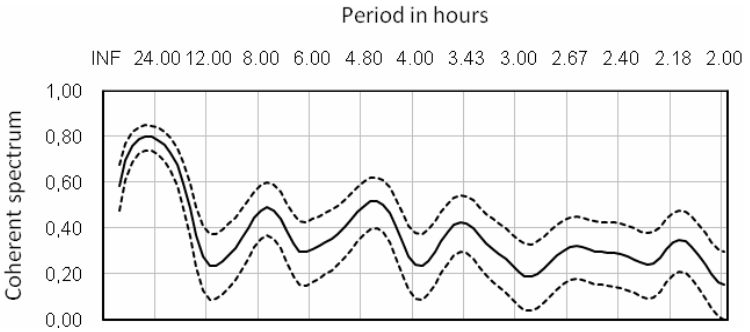

Fig. 9a. Absolute coherency spectrum for the Ozone (ppb) and Relative Humidity (%) time series.

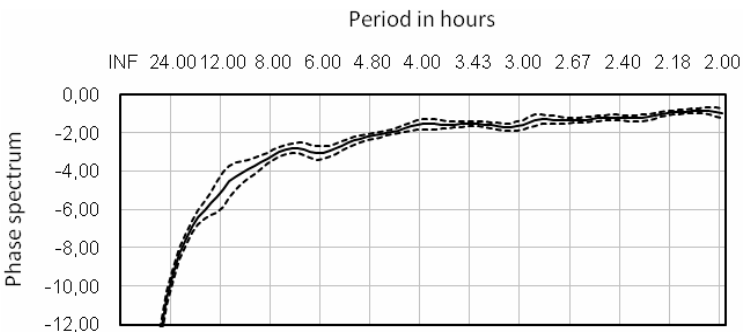

Fig. 9b. Phase spectrum for the Ozone (ppb) and Relative Humidity (%) time series.

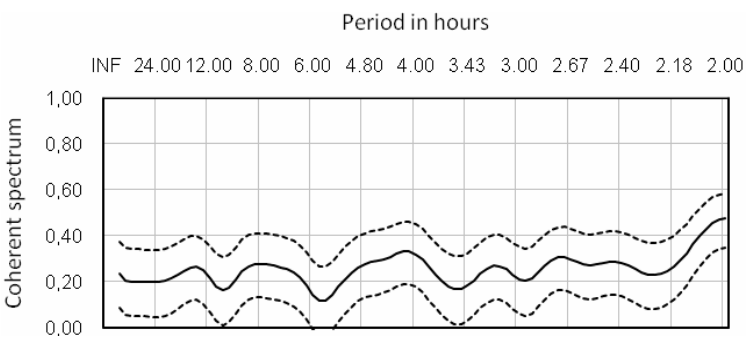

Fig. 10a. Absolute coherency spectrum for the Aerosols (LPC-based particle concentrations) and Relative Humidity (%) time series.

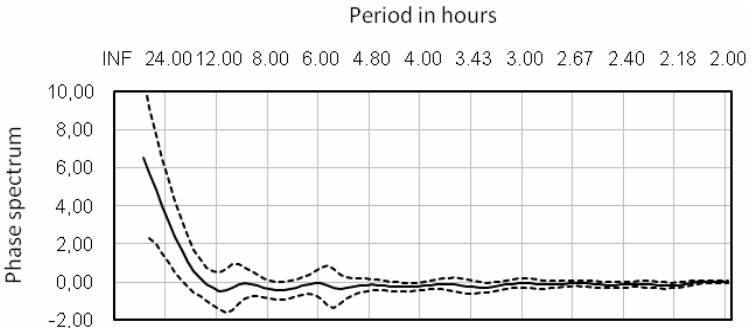

Fig. 10b. Phase spectrum for the Aerosols (LPC-based particle concentrations) and Relative Humidity (%) time series.

The LPC – wind velocity pair. The results obtained by running cross-spectrum analysis for the pair aerosols and wind velocity did not show good coherence (Fig.11a). For shorter periods (2.5 hour) the coherence is statistically weak. The particle-concentration's phase lag is 2 hours for this period (Fig.11b).

The ozone – aerosol pair. As discussed above, relationships between the aerosol-particle concentrations, as measured by the LPC, and ozone are of special interest. However, and as expected from the introductory analysis above, the results of our spectral analysis provide only limited information. There is no statistically significant coherence (> 0.2, within the confidence interval) for the parameters in any of the periods (cf. Fig. 12a). The coherence spectrum suggests that periodic patterns do not occur in the time series for this pair. The phase spectrum (Fig. 12b) shows a non-constant lag, reaching 8 hours for the 24-hours period.

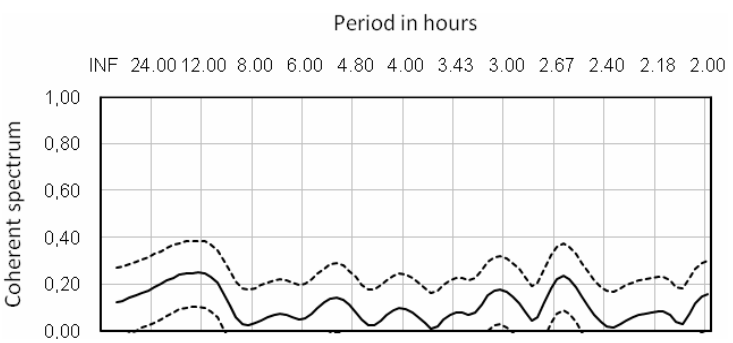

Fig. 11a. Absolute coherency spectrum for the Aerosols (LPC-based particle concentrations) and Wind-speed (ms^{-1}) time series.

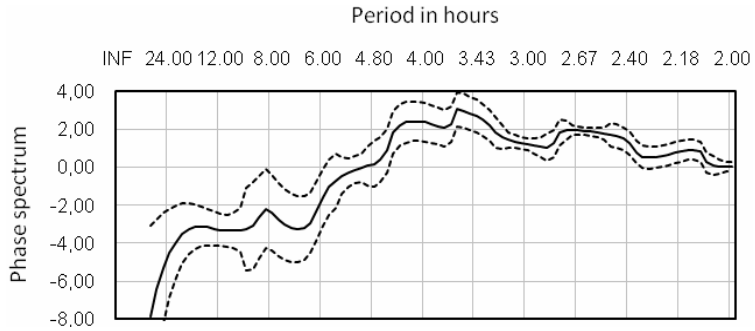

Fig. 11b. Phase spectrum for the Aerosols (LPC-based particle concentrations) and Wind-speed (ms^{-1}) time series.

Additional observations. We also carried out spectral analysis for other combinations of the data (graphs not shown here). The results obtained by running cross-spectrum analysis for the pair aerosols and temperature did not present any statistically significant values. The coherence spectrum showed the coherence of the two parameters to be above the statistically significant minimum coherence for the 24 hour period only. That makes further analysis of the spectra obtained for this period statistically non-representative. This threshold is determined by the length of the time series and in this case is about 0.2. The phase spectrum showed that for periods longer than 12 hours, particle concentrations essentially lag behind the temperature, reaching a difference of 6 hours for a 24-hours cycle. The diurnal variations graphics (see Fig. 2) showed that the aerosols' maximum is (on the average) around noon, after which the quantity sharply decreases. The temperature, however, is at its maximum in the afternoon, between 1 and 6 p.m. Hence, aerosols do not relate clearly to temperature, although exhibiting a weak dependency on this meteorological parameter for the 24-hour period.

The ozone-temperature pair (graphs not shown here) showed a relatively smooth power spectrum with a single peak for the 24 hour period – an obvious daily trend. There is an accumulation of power for the temperature time series for the 24-hours period too, but there is a leakage of power in the 7, 5, and 3.5 hour periods, presented by few smaller peaks. The coherence of the two parameters is very good (above 0.8) for the 24-hours period. A few coherences with smaller values (between 0.35 and 0.5) were noticed for the 7, 4.5, 3.5, and 2.75 hours periods. Slow runs of the ozone from the temperature in the phase by 2 hours were found for the 12 and 24 hour periods. For the other periods the difference was smaller. For periods shorter than 6 hours the ozone and the temperature are almost synchronous. The coherence and the slight phase shift are also obvious in the daily trends. Typically, the ozone-temperature pair is almost synchronous for periods shorter than 6 hours, and for a 24-hours period the ozone lag is only 4 hours. Also, the coherence for the twenty-four-hour period (0. 8-0. 9) was strong.

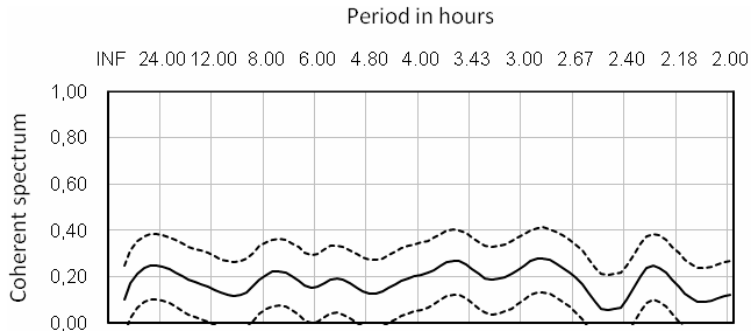

Fig. 12a. Absolute coherency spectrum for the Ozone (ppb) and Aerosols (LPC-based particle concentrations) time series.

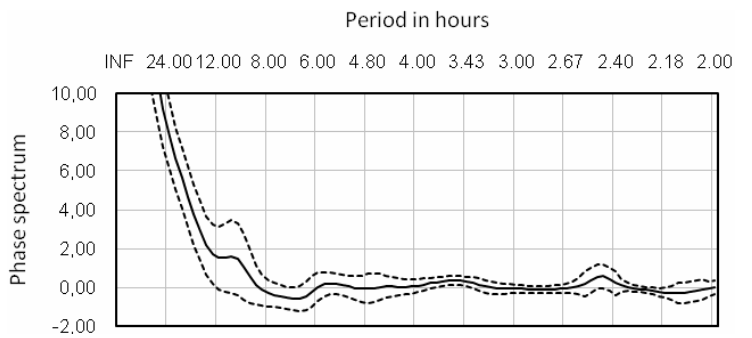

Fig. 12b. Phase spectrum for the Ozone (ppb) and Aerosols (LPC-based particle concentrations) time series.

Summary and conclusions

In this contribution we have presented and examined an extensive sequence (covering nearly 1900 hours) of coastal data on meteorological parameters, ozone concentrations, and concentrations of aerosol particles larger than 0.5 μm. Introductory statistical analyses of the data set suggested a number of potential interrelationships, and phase-shifts, between ground-near ozone concentration variations and some meteorological parameters (solar radiation and temperature in particular). Aerosol-particle concentrations (and fluxes) showed some connections with wind speed and wind direction, and also with solar radiation; the latter relationship however likely to be a result of the partly radiation-driven pattern for wind speed and direction.

These introductory findings warranted the use of Mathematical Spectral Analysis in processing time series for meteorological applications. The conclusions based on the power spectra, the cross-amplitude spectrum, the absolute coherency spectrum and the

phase spectrum are confirmed by the diurnal cycles.

The ozone and the meteorological parameters examined here show good correlations making the strong inter-dependence between the ozone-driving processes and meteorology evident.

In contrast to ozone, the particle-number concentrations do not relate to other parameters in a clear manner. However, the quantity has a weak dependency on the meteorological parameters for the 24-hour period and a little stronger for shorter periods (8 hours), especially with the relative humidity factor which aerosol-particle concentrations follow not far behind. This might be linked to inflows of humid air mass from the sea and dry air from the mainland, inasmuch the size of hygroscopic sea-salt aerosol particles is RH-dependent. That is, the particle-size distribution may shift in and out of the size range recorded by the LPC. This suggests that the 8–hour cycle best describes the aerosol concentration-variation patterns.

We found that the number-concentrations of aerosol particles in the size range studied here (> 0.5 μm) do not show clear relations with RH and temperature, while the ozone time series are well correlated with meteorological parameters for a 24-hours period. Interestingly, however, aerosols better relate to RH for an 8-hour period which we believe is due to the geographical situation of the site and the daily wind patterns in combination with the RH-effects on aerosol-particle hygroscopicity.

Relationships between ozone concentrations and particle concentrations may exist, but, if so, are not clearly brought out in this data set. Instead, our data suggest that such interactions are weak in particle-size ranges above 0.5 μm (i.e., in size ranges captured by the LPC deployed in this study).

The above findings demonstrate that mathematical spectral analysis (revealing spectra for power, cross-amplitude, absolute coherency, and phase) is a forceful modern statistical tool for finding cycles and inter-dependencies amongst meteorological and physic-chemical data.

Acknowledgments: The authors are grateful for the financial support from the National Science Fund contracts ВУ НЗ-03/05 and DO 01-127/08 at the Ministry of Science and Education, Bulgaria. We also gratefully acknowledge the support by the Linneaus University Faculty Board of Natural Sciences, and the contributions by the IEDA Project, funded by the Swedish Council for Planning and Coordination of Research (FRN) and the Swedish Research Council (VR).

References

Alexandrov V.D., Velikov S.K., E.H. Donev E.H., Ivanov D.M. (2005) Quantifying nonlinearities in ground level ozone behavior at mountain-valley station at Ovnarsko, Bulgaria by using neural networks. Bulgarian Geophysical 2005, vol. 31. 1-4

Andreae M.O., Crutzen P.J. (1997) Atmospheric aerosols: biogeochemical sources and role in atmospheric chemistry. Science 276, 1052-1059.

Bonasoni P., Cristofanelli P., Calzolari F., Bonafé U., Evangelisti F., Stohl A., Zauli Sajani S., van Dingenen, Colombo R.T., Balkanski Y. (2004) Aerosol-ozone correlations during dust transport episodes. Atmos. Chem. Phys. 4, 1201-1215.

Brockwell P.J., Davis R.A. (1991) Time Series: Theory and Methods (2nd edition). Springer, Heidelberg.

Donev E. (1977) Приложение на математическия спектрален анализ при изследване на временни редове в метеорологията. Хидрология и метеорология, год. XXVI, кн.5.

Donev E., Petrova L. (1979) Спектры метеорологических элементов в приводном слое атмосферы тропической зоны Индийского океана. Сборник трудов "Мусон-77", Гидрометеоиздат.

Donev E. (1986) Спектрални оценки на късопериодичната изменчивост с времето на някои замърсители на въздуха. Годишник на СУ, том 79.

Donev E., Zeller K., Avramov A. (2002) Preliminary background ozone concentrations in the mountain and coastal areas of Bulgaria. Environmental Pollution 117, 281-286.

Foltescu V.L., Pryor S.C., Bennet C. (2005) Sea salt generation, dispersion and removal on the regional scale. Atmospheric Environment 39, 2123–2133.

Fowler D., Pilegaard K., Sutton M.A., et al. (2009) Atmospheric composition change: ecosystems–atmosphere interactions. Atmospheric Environment 43, 5193–5267.

Houthuijs D., Breugelmans G., Hoek G., Vaskövi E., Mihailikova E., Pastuszka J.S., Jirik V., Sachelarescu S., Lolova D., Meliefste K., Uzunova E., Marinescu C., Volf J., de Leeuw F., van de Wiel H., Fletcher T., Lebret E., Brunekreef B. (2001) PM10 and PM2.5 concentrations in Central and Eastern Europe: results from the Cesar study. Atmospheric Environment 35, 2757-2771.

IPCC (2007): Climate Change 2007: The Physical Science Basis. Contribution of Working Group I to the Fourth Assessment Report of the Intergovernmental Panel of Climate Change [Solomon, S., et al. (eds)]. Cambridge University Press, Cambridge, U.K.

Karnosky D.F., Percy K.E., Chappelka A.H., Simpson C., Pikkarainen J. (eds) (2003) Air Pollution, Global Change and Forests in the New Millenium. Elsevier, Amsterdam.

Knipping E., Dabdud D. (2003) Impact of chlorine emissions from sea-salt aerosol on coastal urban ozone. Environmental Science and Technology 37, 275-284.

Paulot F., Crounse J.D., Kjaergaard H.G., Kürten A., St. Clair J.M., Seinfeld J.H., Wennberg P.O. (2009) Unexpected epoxide formation in the gas-phase photooxidation of isoprene. Science 325, 730-733.

Priestley M.B. (1981) Spectral Analysis and Time Series. Academic Press, New York.

Seinfeld H., Pandis S.N. (1998) Atmospheric Chemistry and Physics. John Wiley & Sons Inc, New York.

Skakalova T.S., Savov P.B., Grigorov I.Y., Kolev I.N. (2003) Lidar observation of breeze structure during the transition periods at the Southern Bulgarian Black Sea coast. Atmospheric Environment 37, 299-311.

Whitby K.T. (1978) The physical characteristics of sulfur aerosols. Atmospheric Environment 12, 135-161.

Wiman B.L.B, Unsworth M.H., Lindberg S.E., Bergkvist B., Jaenicke R., Hansson H-C. (1990) Perspectives on aerosol deposition to natural surfaces: interactions between aerosol residence times,

removal processes, the biosphere and global environmental change. Journal of Aerosol Science 21, 313–333.

Wiman B.L.B., Donev E., Yurukova L., Gaydarova P.N. (1999a) Integrated Diagnosis and Assessment (IEDA) project: objectives and strategies. Journal of Balkan Ecology 2, 5-11.

Wiman B.L.B., Donev E., Yurukova L., Gaydarova P.N. (1999b) Integrated Environmental Diagnosis and Assessment (IEDA) project: methods, measurements and results for project introductory phase, spring-autumn 1998. Journal of Balkan Ecology 2, 17-27.

Wiman B.L.B. (2000) Aerosols at air/water/land interfaces: modeling and measurements. In: Gryning S-E., Batchvarova E. (eds) Air pollution modelling and its application, Vol XIII. Kluwer

Academic/Plenum Publishers, New York, pp. 687–698.

Wiman B.L.B., Velchev K., Gaydarova P.G., Donev E.H., Yurukova L.D. (2002) A note on aerosol mass-versus-size distributions in the south-east Bulgarian Black Sea coastal region. Bulgarian Journal of Meteorology and Hydrology 13, 1-2, 26-39.

Wiman B.L.B, Donev E.H., Nikolova P.N., Yurukova L.D. (2007) Aerosol-borne trace elements in Bulgaria: concentration levels in coastal and mountainous regions. Bulgarian Geophysical Journal 33, 3-19.

Wiman B.L.B., Gaydarova P.N. (2008) Spectral composition of shade light in coastal-zone oak forests in SE Bulgaria, and relationships with leaf area index: a first overview. Trees 22, 63–76 [DOI 10.1007/s00468-007-0169-4]

Zeller K., Zimmerman G., Hehn T., Donev E., Denny D., Welker J. (2001) Analysis of inadvertent microprocessor lag time on eddy covariance results. Journal of Applied Meteorology 40, 1640-1646.

Седемдесет и девет дневни времеви редове от измервания на озон, аерозоли и метеорологични параметри: статистически връзки и изводи

Данко М. Иванов, Деян Г. Лазаров, Ангел П. Благоев, Венцислав Ц. Данчовски, Евгени Х. Донев и Бо Л. Б. Уиман

Резюме: В тази работа се прилагат разнообразни статистически методи с цел да се изследват връзките между времеви редове от измерени концентрации на приземен озон, аерозоли (концентрация на аерозолни частици, по-големи от 0.5μm) и метеорологични параметри. Времевите последователности са получени автоматично и едновременно (записи на средночасовите стойности) от крайбрежна станция в близост до Ахтопол, България за периода 10 май - 27 юли 2002-ра година. Първоначалният статистически анализ показва множество потенциални връзки между вариацията на концентрацията на приземен озон и някои метеорологични параметри. Също така, данните показват известни връзки между концентрациите на аерозоли, посоката на вятъра и слънчевата радиация. Втората връзка е възможно да бъде обяснена с частичното активиране на циркулацията на вятъра от страна на радиацията. Тези първоначални заключения са потвърдени от спектралния математически анализ (СМА) приложен към времевите редове, с което се показва полезността на СМА отнесен към метеорологичните приложения. Изводите основаващи се на спектралната плътност, амплитудите на взаимните спектри, спектрите на абсолютна кохерентност и фазовия спектър са потвърдени от денонощните цикли. Спектралната плътност на наблюдаваните данни, взаимните спектри, спектрите на абсолютна кохерентност и фазовия спектър са изчислени на база едночасовите стойности на метеорологичните параметри, данните за аерозолите и озона. Настоящия труд съдържа изчислените спектри и тяхното взаимно представяне. Едно от заключенията е, че денонощните вариации на метеорологичните параметри добре обясняват денонощните вариации в концентрацията на озон, като дневните вариации в концентрацията му по-слабо се влияят от изменчивостта на метеорологичните параметри.